Thulium Optical Lattice Clock With Zeeman-Insensitive Synthetic Clock Frequency

Tregubov D., Golovizin A., Provorchenko D.,
Mishin D., Khabarova K., Sorokin V.,
Kolachevsky N.
P.N. Lebedev Physical Institute
Moscow, Russia

Khabarova K., Kolachevsky N.
Russian Quantum Center
Moscow, Russia

***Abstract*—In this work we discuss interrogation scheme required for the use of synthetic frequency in thulium optical lattice clock and underlying specifics of servo signal generation. In order to achieve insensitivity of the synthetic frequency to periodic oscillations of the magnetic field, simultaneous interrogation of two clock transitions is beneficial, which complicates optimization of digital lock parameters and may result in crosstalk. We used numerical simulations to test the performance of digital locks and verify absence of systematic frequency shifts related to the interrogation scheme.**

Keywords— metrology, optical clock, thulium, simulation

I. INTRODUCTION

Optical clocks nowadays reach fractional instability and uncertainty of 10^{-18} and better [1]. In order to achieve this, precise control of environmental parameters that create undesired and often large systematic frequency shift is required. For the neutral atoms based optical clock, these are the control of the thermal surrounding of the atomic cloud, lattice Stark shift and, to a lesser degree, quadratic Zeeman shift. Recently [2], we have showed that total systematic frequency shift in thulium optical clock is expected to be extremely small due to low static polarizability of 1.14 μm clock transition and the use of synthetic frequency. Since two hyperfine levels of the ground (clock) state (Fig. 1) experience almost equal but opposite in sign second-order Zeeman shift, synthetic frequency $\nu_s = (\nu_{43} + \nu_{32})/2$ is insensitive to Zeeman shift. This significantly relaxes the requirements on environmental conditions and opens up a possibility of a robust transportable thulium optical clock. While the low static polarizability is a convenient property of the clock transition, the synthetic frequency requires an unconventional operating scheme where we interrogate two clock transitions simultaneously.

In order to check for possible undesired systematic frequency shifts resulted from this interrogation method, we used numerical simulations. These simulations also helped us discover digital lock parameters that optimize the clock performance. Here we discuss in details the numerical simulations, systematic frequency shifts resulted from the interrogation method, and search for optimal feedback parameters to lock both clock transitions at once, that is required by the synthetic frequency scheme.

II. METHODS

In order to use the synthetic frequency in thulium optical clock, we need to interrogate two clock transitions between different hyperfine levels. There are two ways of approaching this (Fig. 2). The first one is a sequential interrogation scheme, where we can use two experiment cycles to interrogate both clock transitions separately. This method works in many other clock interrogation schemes when two different Zeeman sublevels are interrogated for the first order Zeeman shift cancelation. There is no influence of one clock transition excitation on the other, as they are separated in time. This can be used for benchmarking the performance of the method that we are using experimentally. The second approach is a simultaneous interrogation scheme as it was presented in [2]. The main advantage of this scheme is complete suppression of the Zeeman effect, and exactly simultaneous excitation of clock transitions is essential here. Hence, unwanted influence of one transition on another is inevitable and has to be taken into account. Another advantage of this method is that we get twice more data about our system per unit of time which allows us to lock the laser to atoms more tightly.

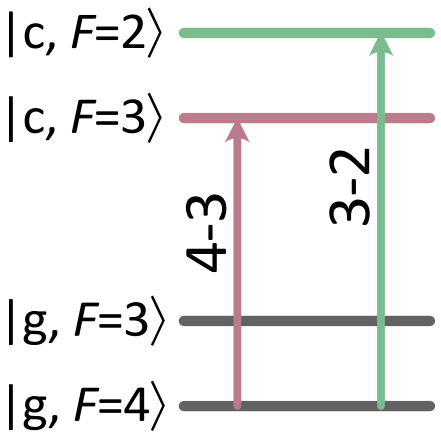

Fig. 1. Energy levels in Tm relevant to the 1.14 μm clock transition. g – ground level, c – upper level of the clock transitions, *F* – total angular momentum. The two clock transitions between hyperfine components, denoted as "4-3" and "3-2", are used in the synthetic frequency method.

978-1-6654-3935-0/21/$31.00 ©2021 IEEE

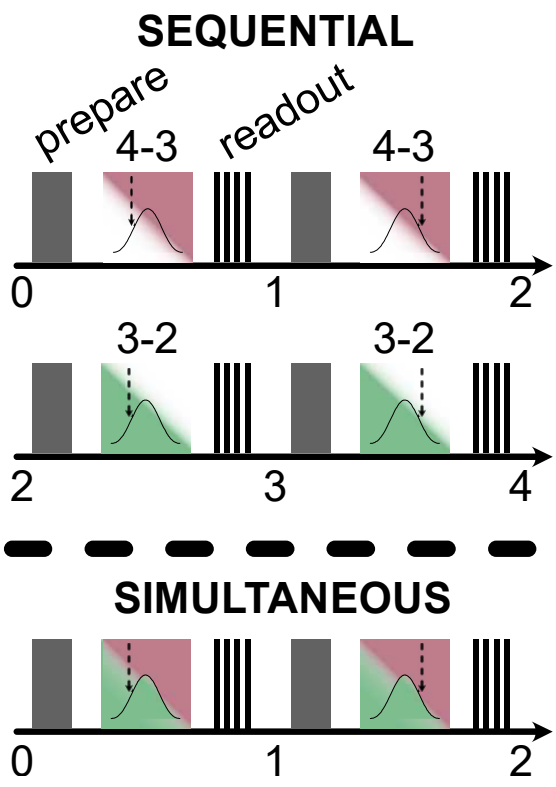

Fig. 2. Sequential (top) and simultaneous (bottom) interrogation schemes that may be used for synthetic frequency method in Tm optical clock. Horizontal axis illustrates time with labels indicating number of single measurement cycles before the process repeats periodically. For each transition (4-3 and 3-2) it is necessary to measure excitation probability on both left and right slopes of the spectrum before calculating error signal.

We created three separate entities in our numerical simulations for better representation of actual experiment: (i) a laser that generates light to excite clock transitions, (ii) atoms that are described as many-level quantum systems, and (iii) a setup manipulator that controls excitation and measurement procedures and digital locks. Here, we will describe each of these systems one by one.

The laser in our numerical simulations is responsible for generation of noisy signal related to frequency of the probe radiation that we use to excite clock transitions. In our simulations, we consider white-noise for phase, and random-walk-noise for frequency which is always present in our setup. In the experiment, we use PDH method to stabilize the clock laser to a 75 mm-long ULE cavity, and we achieve its spectral linewidth of less than 6 Hz [3,4] (the RMS amplitude of the white phase noise in the model). The ULE cavity is subjected to long-term drifts due to aging and temperature fluctuations, which is captured in the modelling as frequency random-walk. This is the noise that we try to negate using servo signal with our digital lock. We used noise parameters that, together with other sources described below, produce frequency signals close to experimentally observed, both in timescale and amplitude. For example, the frequency random-walk that describes our system is tens of Hz on a timescale of several hours. For better representation of the setup, we introduced long-term power fluctuations to account for gradual misalignments and acousto-optical modulators (AOMs) temperature changes.

The atoms in our numerical simulations are responsible for all particle-related noise and sensitivity to the environment. First of all, their finite number imposes quantum projection noise (QPN) each time the setup manipulator performs a measurement. Apart from QPN, we add gaussian distribution of the number of atoms during magneto-optical trap (MOT) loading and of the optical pumping efficiency to two initial quantum states [5]. We can also change frequency of each if the two clock transitions for all the atoms in order to introduce influence of the magnetic field. Essential part of the experiment is clock transition excitation and readout which we tried to emulate by describing atoms as many-level quantum systems. We accounted for all magnetic sublevels for each hyperfine components of clock transition's ground and upper levels, 28 magnetic sublevels in total. In order to calculate their evolution in time during the experiment cycle, we used a python module QuTiP [6]. Since simulations of many-level quantum systems generally take a long time, we precalculated atom's state evolution for key processes in our experiment. Namely, for 80-ms-long excitation (any of the two clock transitions or both are excited), free evolution before and during the readout process, and 1 or 2-ms-long de-excitation that we use in the readout process.

The third entity in our simulations is the setup manipulator that makes use of both laser and atoms and performs actions close to those in real experiment. First of all, it emulates MOT loading by sampling initial number of atoms from gaussian distribution, and optical pumping by randomly selecting a fraction of them that are successfully transferred to the desired state, or lost. The next step is 80-ms-long clock transition excitation where it takes the current laser power and compares its frequency to those of atoms. Here, the setup manipulator uses the clock transition excitation on left or right slopes of the excitation spectrum by alternating between additional frequency shift of +5 Hz or –5 Hz.

The readout procedure is simulated with the setup manipulator as well. It consists of 4 steps (Fig. 3), and during each step we use destructive measurement of atoms in the ground state:

1. Measure number of atoms in the ground state F=4. This produces number of atoms which are not excited by the clock transition 4-3, with some adjustments. These atoms leave the experiment after destructive measurement.
2. Wait 7-8 ms, then measure number of atoms in the ground states F=4 and F=3. This produces number of atoms which are not excited by the clock pulse 3-2, with some adjustments.
3. Apply 1- or 2-ms-long pulse to transfer atoms from upper clock states to the ground ones. This action's fidelity changes every cycle according to the clock laser power and frequency.
4. Repeat steps 1 and 2 that will produce number of atoms excited by the relevant clock transition.

During wait time between these steps we always calculate free evolution of atomic state, since the wait time of 7-8 ms is not very small as compared to the upper clock level lifetime of 120 ms [7].

The experiment cycle ends here, and after two of these (on the left and right slopes), the setup manipulator calculates an error signal. It generates servo signal according to proportional (P) and integral (I) parameters of the digital lock and applies it to "AOMs" (used to introduce additional frequency shifts separately for both clock transitions).

III. RESULTS

Similar to the actual experiment, before doing simulations we found calibration parameters that allowed us to calculate excitation probabilities from the 4 numbers (described above) that we get in each experiment cycle and calculate the error signal. First, we turned all the noise off in the simulations and scanned frequency of the clock laser. Then we adjusted coefficients to minimize influence of one clock transition (4-3) on the readout numbers of the other (3-2). Together with turning noise sources back on, we also introduced errors in calibration coefficients by drawing them from a gaussian distribution with 10% standard deviation from the ideal value for each simulation run.

First, we searched a wide range of parameters to find areas where we are sure the digital lock is stable. We searched a grid of 20x20 values of P and I parameters with averaging of 5 different "day-long" experiments for each pair. We did this for both excitation schemes, simultaneous and sequential (Fig. 3), as we want to compare them later. We identified regions with the lowest instability of the clock frequency (hot areas in Fig. 3). During these simulations, we also confirmed that there is no systematic frequency shift, at least related to the used method. Histogram of the difference in mean frequency can be seen on Fig. 4. At this point, we did not yet introduce magnetic field fluctuations or other shifts of the clock transition caused by interaction with the environment.

In the next step we confirmed the main advantage of synthetic frequency by numerical simulations (Fig. 5). We introduced magnetic field fluctuations by adding opposite frequency shifts for 4-3 and 3-2 clock transitions. Here we used harmonics of different periods as well as random-walk noise.

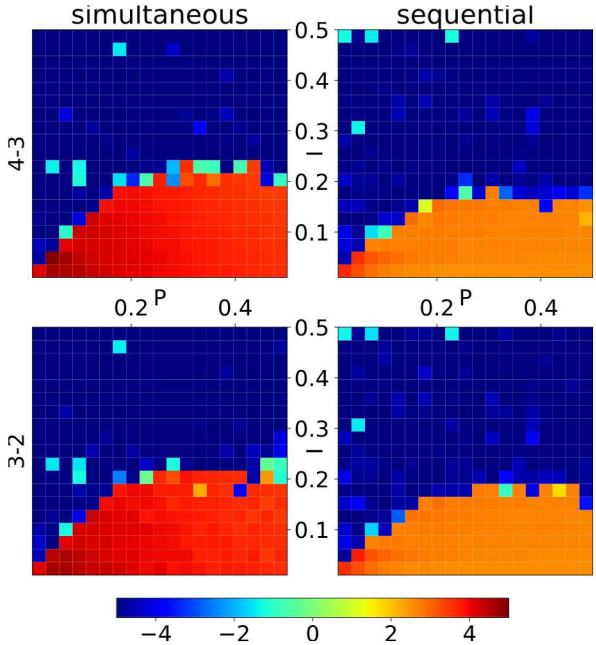

Fig. 4. Digital lock performance for simultaneous (left column) and sequential (right column) scheme. Results are presented separately for 4-3 (top row) and 3-2 (bottom row) clock transitions. We searched a wide area of digital lock parameters: proportional coefficient P (*x*-axis) and integral coefficient I (*y*-axis). The heatmap illustrates negative power of 10 for the final Allan deviation written in Hz.

IV. DISCUSSION

According to the results of the search for optimal parameters, it is clear that the simultaneous clock excitation scheme is generally better. However, we should compare the schemes at optimal P and I parameters for each scheme. On average, we see that the performance of simultaneous scheme is ~1.5 times better than that of sequential. This is an expected result as we are using 2 times lower period of servo loop and apply the feedback twice more frequently. Here we assume that we are limited by the laser noise, but not by the QPN.

Introducing magnetic field fluctuations with frequencies that are odd-multiple of 4 single-measurement cycles rate (Fig. 5) reveals that only sequential scheme suffers from a significant frequency shift of tens of mHz. This result can be explained if we look at times when the clock transition excitation takes place along with Zeeman frequency shifts of both clock transitions. This is similar to the Dick effect [8], only resulting from the magnetic field fluctuations. Fluctuations at harmonics with such frequencies might always be present, and the simultaneous interrogation scheme conveniently compensates them.

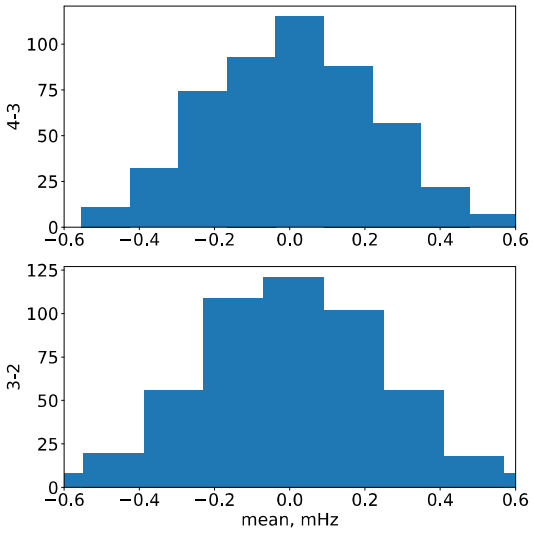

Fig. 3. Histogram of frequency shift difference between simultaneous and sequential scheme for 500 simulations, each had "duration" of 4 days, presented separately for 4-3 and 3-2 clock transitions. The shift is less than statistical uncertainty 0.2 Hz of individual measurement, which confirms that the crosstalk between digital locks for 4-3 and 3-2 clock transitions is negligible.

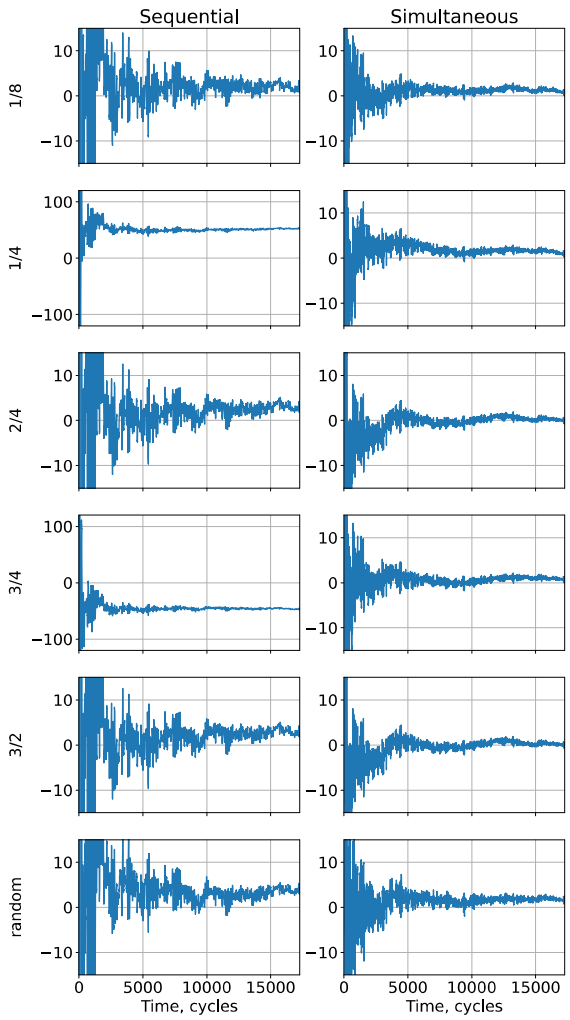

Fig. 5. Results of cumulative frequency averaging (in mHz) over time (in measurement cycles) for sequential and simultaneous scheme for different magnetic field fluctuations. The labels on the left side correspond to harmonic frequency of magnetic field fluctuations in measurement cycle rates, and the last plots are for random walk of magnetic field.

V. Conclusions

In this work, using numerical simulations we showed that the synthetic frequency with simultaneous clock transition excitation scheme allows us to negate influence of Zeeman shift resulting from magnetic field fluctuations without introducing any additional systematic shifts. The simulations helped us with a search for optimal feedback parameters of digital lock which usually takes a long time experimentally. The scheme itself requires initial calibration, but after that may be readily used. We have already used this technique in our experiments for suppression of Zeeman shift, observing zero shift of the synthetic frequency within our current statistical uncertainty $\sim 3 \times 10^{-17}$.

Acknowledgment

Authors acknowledge support from RSF grant #19-12-00137.

References

[1] A. D. Ludlow, M. M. Boyd, J. Ye, E. Peik, and P. O. Schmidt, “Optical atomic clocks,” Rev. Mod. Phys., vol. 87, no. 2, pp. 637–665, 2015.

[2] A. Golovizin et al., “Extraordinarily low systematic frequency shifts in a bicolor thulium optical clock”, Nat. Commun., in press.

[3] A. Golovizin et al., “Ultrastable Laser System for Spectroscopy of the 1.14 μm Inner-Shell Clock Transition in Tm and Its Absolute Frequency Measurement,” J. Russ. Laser Res., vol. 40, no. 6, pp. 540–546, Nov. 2019.

[4] A. Golovizin et al., “Inner-shell clock transition in atomic thulium with a small blackbody radiation shift,” Nat. Commun., vol. 10, no. 1, pp. 1–8, Dec. 2019.

[5] E. Fedorova et al., “Simultaneous preparation of two initial clock states in a thulium optical clock,” Phys. Rev. A, vol. 102, no. 6, p. 63114, Dec. 2020.

[6] J. R. Johansson, P. D. Nation, and F. Nori, “QuTiP 2: A Python framework for the dynamics of open quantum systems,” Comput. Phys. Commun., vol. 184, no. 4, pp. 1234–1240, Apr. 2013.

[7] D. Sukachev et al., “Inner-shell magnetic dipole transition in Tm atoms: A candidate for optical lattice clocks,” Phys. Rev. A, vol. 94, no. 2, p. 22512, Aug. 2016.

[8] A. Quessada, R. P. Kovacich, I. Courtillot, A. Clairon, G. Santarelli, and P. Lemonde, “The Dick effect for an optical frequency standard,” J. Opt. B Quantum Semiclassical Opt., vol. 5, no. 2, p. S150, Apr. 2003.